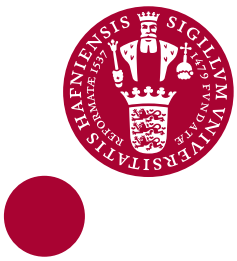

Comparable effects of manure and its biochar on reducing soil Cr bioavailability and narrowing the rhizosphere extent of enzyme activities

Liu, Shibin; Pu, Shengyan; Deng, Daili; Huang, Hongyan; Yan, Chun; Ma, Hui; Razavi, Bahar S.

Published in:
Environment International

DOI:
10.1016/j.envint.2019.105277

Publication date:
2020

Document version
Publisher's PDF, also known as Version of record

Environment International 134 (2020) 105277

Contents lists available at ScienceDirect

Environment International

journal homepage: www.elsevier.com/locate/envint

Comparable effects of manure and its biochar on reducing soil Cr bioavailability and narrowing the rhizosphere extent of enzyme activities

Shibin Liu[a,b,1], Shengyan Pu (PhD)[a,c,*], Daili Deng[a,1], Hongyan Huang[a], Chun Yan[a], Hui Ma[a,d], Bahar S. Razavi[e]

[a] State Key Laboratory of Geohazard Prevention and Geoenvironment Protection (Chengdu University of Technology), 1# Dongsanlu, Erxianqiao, Chengdu 610059, Sichuan, PR China
[b] College of Earth Sciences, Chengdu University of Technology, 1#Dongsanlu, Erxainqiao, Chengdu 610059, Sichuan, PR China
[c] State Key Laboratory of Environmental Criteria and Risk Assessment, Chinese Research Academy of Environmental Sciences, Beijing 100012, PR China
[d] Department of Plant and Environmental Sciences, University of Copenhagen, Thorvaldsensvej, 401871 Frederiksberg, Denmark
[e] Department of Soil Science and Plant Nutrition, University of Kiel, Kiel, Germany

ARTICLE INFO

Handling editor: Da Chen

Keywords:
Soil zymography
Heavy metal
Soil contamination
Enzyme activities
Manure
Biochar
Rhizosphere

ABSTRACT

Chromium (Cr) contamination is especially hazardous to soil biota. Application of manure and biochar has been frequently proposed to remediate Cr-contaminated soil. However, the understanding of mechanisms behind manure and biochar impacts on soil enzyme activities requires advanced visualization technologies. For the first time, we compared manure and its biochar influence on the spatial distribution of β-glucosidase, N-acetyl-glucosaminidase and phosphomonoesterase activities in Cr-contaminated soil using direct zymography. Maize was planted for 45 days in (a) soil mixed with manure, (b) soil mixed with manure-derived biochar and (c) soil without any addition. Soil pH decreased over 45 days, inducing an increase in acid soluble Cr. The concomitant decrease in β-glucosidase and N-acetyl-glucosaminidase activities explained the narrowing rhizosphere extent of enzyme activities by 13–44%, indicating that increased Cr bioavailability decreases microbial activities. A larger maize performance index and the greatest plant shoot/root ratio after biochar application suggested enhanced maize growth ($p < 0.05$). In contrast, manure induced the narrowest extent of β-glucosidase and phosphomonoesterase activities due to the addition of labile organic compounds and nutrients following its application. Our study emphasizes the importance of pH on Cr bioavailability and enzyme activities and demonstrates that biochar application is more ideally suited for remediating Cr-contaminated soil.

1. Introduction

Soil contamination with chromium (Cr) has gained substantial attention worldwide because of the high risk of inducing hazardous consequences (Shahid et al., 2017). For instance, Cr contamination alters soil microbial community structure and activities, and depresses plant growth and development (Mallick et al., 2010; Carpio et al., 2018; Ertani et al., 2017). The influence of Cr on plant growth is much stronger in the rhizosphere (e.g., a small volume up to a few millimeters surrounding living roots) compared to bulk soil (Hinsinger et al., 2009; Antoniadis et al., 2017a). The rhizosphere contains various rhizodeposits released by roots, which stimulate microbial activities and enzyme production and form one of the most dynamic and intense hotspots of enzyme activities in terrestrial ecosystems (Bais et al., 2006; Oburger et al., 2014). Through the rhizosphere, excessive Cr may inhibit plant growth by decreasing chlorophyll content, depressing plant growth and inhibiting germination (Rizvi and Khan, 2018).

Enzymes are the main biological drivers of soil carbon and nutrient cycling processes and an early indicator of soil microbial and root activities to reflect the impact of heavy metal contamination (Sinsabaugh et al., 2008). Sharp gradients are formed for rhizosphere enzyme activity and typically demonstrate a sigmoidal curve (Kuzyakov and Razavi, 2019). The distance from the root center to bulk soil where enzyme activities become stable has been generally defined as the rhizosphere extent of enzyme activity. Many previous studies have focused on visualizing the rhizosphere extent of enzyme activity using the *in situ* zymography techniques (Razavi et al., 2016; Liu et al., 2017; Pu et al., 2019). For instance, the rice rhizosphere extent of enzyme

* Corresponding author at: State Key Laboratory of Geohazard Prevention and Geoenvironment Protection (Chengdu University of Technology), Chengdu 610059, PR China.
E-mail addresses: pushengyan13@cdut.cn, pushengyan@gmail.com (S. Pu).
[1] The authors declare that there is no conflict of interests regarding the publication of this paper. S. Liu and D. Deng contributed equally to this work.

https://doi.org/10.1016/j.envint.2019.105277
Received 5 August 2019; Received in revised form 9 October 2019; Accepted 16 October 2019
Available online 11 November 2019

activities in response to phosphorus and cellulose applications has been investigated (Wei et al., 2018). The total enzymatic hotspot area for the whole soil profile as affected by multiple heavy metals was also calculated (Duan et al., 2018).

Regarding the impact of heavy metals, the activities and dynamic behaviors of enzymes are mainly governed by the type, speciation and bioavailability of contaminants (Abdu et al., 2016; Shahid et al., 2017). For instance, Cr(VI) is more toxic to plants and microbes compared to Cr(III) because of its high reactivity with other elements. The potentially mobile fractions, e.g., the exchangeable, reducible, and oxidizable fractions, are considered to be bioavailable (Rinklebe and Shaheen, 2017). Many *in situ* approaches have been used to remediate heavy metal contamination, with the goal of weakening the migration of heavy metals and reducing their bioavailability (Ghosh et al., 2011). Increasing soil organic matter content has yielded promising outcomes with respect to amending Cr-contaminated soil and reducing stress to microbial and root activities (Antoniadis et al., 2017b, 2018; Abbas et al., 2019). For instance, manure is the most commonly used organic fertilizer as it can stabilize heavy metals through various processes such as sorption, reduction, volatilization and rhizosphere modification (Park et al., 2011; Ghosh et al., 2011). In recent years, researchers have also proposed that manure-pyrolyzed biochar not only can enhance remediation of heavy metals, but also promote plant growth (Abbas et al., 2019). Both manure and the biochar involved in remediating Cr-contaminated soils and improving microbial and root activities have their own specific mechanisms (Park et al., 2011; Li et al., 2017). First, although both manure and biochar can immobilize heavy metals by adsorption, promote the formation of soil aggregates and drive heavy metal reduction reactions, the capacities of manure and biochar are diverse and heavy metal-specific (Park et al., 2011; Li et al., 2017; Zhu et al., 2017). Second, the loading of indigenous enzymes and microbes from manure into soil will occur following their application (Criquet et al., 2007), which does not occur with manure-derived biochar. Third, manure and biochar provide organic compounds with various stabilities (Yanardağ et al., 2017). Manure generally maintains easily decomposed organic matters and nutrient contents, while highly recalcitrant aromatic compounds are found in manure-derived biochar (Dinesh et al., 1998; Zornoza et al., 2016). This leads to a trade-off between more complete decomposition and mineralization and the incorporation of these compounds as soil organic matter. Though manure and its biochar have been widely recommended, there is a lack of mechanistic understanding regarding the enzymatic responses of plants and microorganisms to manure and biochar application in Cr-contaminated soil.

Here, we used direct soil zymography to visualize the spatial distribution of enzyme activities on the soil profile. Soil samples were collected from a chromium slag field. Maize (*Zea mays* L.) plants were grown in the rhizoboxes. We compared cow manure with its biochar application using three treatments: 1) Manure: mixed manure throughout the soil; 2) Biochar: mixed biochar throughout the soil; and 3) Control: a control with only soil. The BCR sequential extraction procedure was used to determine the chemical speciation of Cr in soil. Considering the possible diverse impact of Cr for different enzymes, direct soil zymography was used to visualize the spatial and temporal distribution of the activity for the three enzymes: β-glucosidase, phosphomonoesterase and N-acetyl-glucosaminidase. β-glucosidase is responsible for catalyzing the hydrolysis of terminal 1,4-linked β-D-glucose residues from β-D-glucosides and is involved in the carbon (C) cycle (German et al., 2012). Phosphomonoesterase, which catalyzes the hydrolysis of organic phosphorus (P) compounds to inorganic P, is involved in the P cycle (Eivazi and Tabatabai, 1977; Malcolm, 1983). N-acetyl-glucosaminidase (chitinase), which catalyzes the decomposition of chitin to yield low molecular weight chitooligomers, is responsible for C- and nitrogen (N) acquisition (Huang, 2012). We hypothesized that: (1) the application of manure and its biochar will reduce the bioavailability of Cr to varying degrees; (2) the rhizosphere extent of enzyme activities will be wider than the bulk soil hotspots extent of enzyme activities because of the co-release of enzymes by roots and microbes within the rhizosphere (here the bulk soil hotspots were defined as the small volume of bulk soil where microorganisms gather and aggregate (Ekschmitt et al., 2005); (3) the extent will be narrower in manure-treated soil compared to biochar-treated soil due to high nutrient content and the integration of easily decomposed organic compounds.

2. Materials and methods

2.1. Soils, manure and its biochar

Soil samples were collected at a depth of 0–30 cm close to an abandoned chemical plant (105° 31′ 32″ E, 28° 54′ 19″ N, 290 m a.s.l.) located in Luzhou, Sichuan province, China. The chemical plant mainly produced potassium dichromate and was abandoned in 1998. The soil was highly contaminated by Cr because of slag accumulation. Samples were stored in Ziploc bags and immediately transported to the laboratory at Chengdu University of Technology. After removing roots and stones, soil samples were passed through a 2-mm sieve and stored in a 4 °C refrigerator before the subsequent incubation experiment. A small amount of soil was air-dried, milled through a 100-mesh sieve and then prepared for basic physical and chemical analyses.

Cow manure was collected from a farm located in the suburb of Suining, Sichuan province. Manure was spread under a shed, air-dried for two weeks and then passed through a 2-mm sieve for further analysis. Manure-derived biochar was produced from pyrolysis in a temperature-controlled muffle furnace under oxygen-limited conditions. The temperature was ramped at 5 °C min^{-1} up to 420 °C, and held constant for 120 min at 420 °C. After natural cooling, biochar was milled through a 2-mm sieve and used for basic property analysis (Fig. S1). The basic characteristics of soil, manure and biochar are listed in Tables 1 and 2.

2.2. Experimental set-up

This study included three treatments: (1) Manure: mixed manure throughout the Cr-contaminated soil; (2) Biochar: mixed biochar throughout the Cr-contaminated soil; and (3) Control: Cr-contaminated soil without any addition. Manure and its biochar were homogeneously mixed with soil at a dose of 5 g C kg^{-1} soil to ensure that the responses of microbial properties (e.g., enzyme activities) to the additives were intense (Yanardağ et al., 2017). This corresponds to 34 wt-% of C in the soil before manure and biochar application. Preincubation was initiated in triplicate for each treatment by loading fresh samples into 9 rhizoboxes (23 cm × 16 cm × 2 cm), each containing 700 g soil. From the application dose of 5 g C kg^{-1} soil, the amount of manure and biochar added in each rhizobox was 8.97 g and 7.0 g, respectively. Maize (*Zea mays* L.) seeds were surface-sterilized and then germinated in a sterile culture dish for 72 h to ensure plant growth and to avoid fungal

Table 1
Main soil properties and heavy metal content.

Properties*			
Moisture (%)	27.00 ± 0.21	Cr(VI)	150 ± 36.12
pH	5.00 ± 0.01	Cr(T)	2000 ± 64.00
CEC (c mol kg^{-1})	7.90 ± 0.17	Pb	0.33 ± 0.00
EC (μS cm^{-1})	33 ± 0.58	Cu	23.00 ± 21.87
SOM (%)	2.50 ± 0.04	Zn	110 ± 11.43
TN (g kg^{-1})	1.60 ± 0.01	Cd	0.06 ± 0.12
TP (g kg^{-1})	0.33 ± 0.00	Ni	26.00 ± 1.90
MBC (g kg^{-1})	0.22 ± 0.00	As	9.20 ± 0.38

*The unit of all heavy metal is mg kg^{-1}. CEC: cation exchange capacity; EC: electrical conductivity; SOC: soil organic carbon; TN: total nitrogen; TP: total phosphorus; MBC: microbial biomass carbon. Mean ± SE, n = 3.

Table 2
Physicochemical properties of manure and biochar.

Properties	Manure	Biochar
Moisture (%)	0.082 ± 0.005	0.043 ± 0.001
pH	8.60 ± 0.015	9.5 ± 0.033
Ash content (%)	11.0 ± 0.066	27.0 ± 0.46
CEC (c mol kg^{-1})	13.00 ± 0.67	44.0 ± 0.28
Cr (mg kg^{-1})	16.0 ± 1.6	57.0 ± 2.7
Total carbon (%)	39.0 ± 0.30	50.0 ± 0.42
TN (g kg^{-1})	15.0 ± 0.34	26 ± 0.49
TP (g kg^{-1})	2.6 ± 0.12	5.6 ± 0.054
BET ($m^2 \cdot g^{-1}$)	0.95	7.0
Biochar yield	–	30 ± 1.3%

CEC: cation exchange capacity; EC: electrical conductivity; TN: total nitrogen; TP: total phosphorus. BET: Brunauer-Emmett-Teller specific surface area. Biochar yield was calculated by biochar mass/feedstock dry mass × 100%. Mean ± SE, n = 3.

contamination (Sun et al., 2008). Maize was applied in this study because of its fibrous root system which is beneficial for zymography analysis.

Each treatment has three replicates. Nine seedlings close to each other were picked out and transplanted into nine rhizoboxes at a depth of 5 mm. The rhizoboxes were kept inclined at an angle of 45° to make sure the root grows along the lower rhizobox wall (removable) (Razavi et al., 2016). The rhizoboxes were placed in an incubator with a constant temperature of 25 °C, a photosynthetically active radiation intensity of 300 mmol m^{-2} s^{-1} and a daytime of 14 h, which are similar to field conditions during growing season. Soil water content was maintained at 65% of the water holding capacity by maintaining the rhizobox at constant weight with distilled water during the growth period.

Direct zymography was performed at days 5, 15, 30 and 45 as a nondestructive technique to visualize the spatial and temporal patterns of enzyme activities. Samples for soil properties and Cr chemical speciation analysis were taken from part of the rhizoboxes which were not considered for zymography to ensure that zymography analysis was not affected (Hoang et al., 2016). After zymography at day 30, plant shoots were cut off to illuminate the spatial distribution of enzyme activity on the soil profile during root degradation. When the incubation was ended at day 45, the last zymography was applied and then the plant roots were carefully separated from the soil. Rhizosphere soil and bulk (i.e., non-rhizosphere) soil were collected using a needle to compare the distribution of pH and Cr fractions. Rhizosphere soil mainly refers to samples within 4.5 mm away from the root surface (Razavi et al., 2016; Wei et al., 2018; Ma et al., 2018). All visible roots were also picked out from the soil and washed with distilled water to remove soil particles. Both shoot and root biomass were oven-dried at 60 °C for 48 h and then weighted. Maize performance index (PI) was calculated as follows: PI = (dry shoot biomass of plants grown in amendment soil)/(dry shoot biomass of plants grown in control soil). Amendment soil represents Cr-contaminated soils treated with manure or biochar. Control soil represents Cr-contaminated soils without any treatment.

2.3. Soil zymography and imaging procedures

We followed the protocol optimized by Razavi et al. (2016) with a slight modification. Briefly, membranes saturated with 4-methylumbelliferone (MUF)-substrates were used to visualize enzyme activities. The MUF substrates become fluorescent when enzymatically hydrolyzed, and intensities were visilized and quantified under ultraviolet light (Spohn and Kuzyakov, 2013). 4-Methylumbelliferyl-β-D-glucoside (MUF-G), 4-methylumbelliferyl-phosphate (MUF-P) and the MUF-N-acetyl-β-D-glucosaminide (MUF-C) were used as substrates to detect β-glucosidase, phosphatase and N-acetyl-glucosaminidase activity, respectively. All substrates were purchased from Aladdin (China). Each of these substrates was separately dissolved to a concentration of 12 mM in universal buffer (MES buffer, pH: 6.7) (Hoang et al., 2016; Liu et al., 2017). Polyamide membrane filters (i.e., diameter = 20 cm and pore size = 0.45 μm) were cut and adjusted to fit the rhizobox size (i.e., 15.5 × 12.5 cm), then saturated with the specified substrate of each enzyme. The rhizoboxes were opened from the lower, rooted side and the saturated membranes were applied directly to the soil surface (Razavi et al., 2016; Liu et al., 2017). After incubation for one hour, the membranes were carefully stripped from the soil surface, and the attached soil particles were gently removed with a brush. Then, the membranes were placed in a light-proof box and illuminated by ultraviolet (UV) light. The fluorescence from the previous zymography has no effect on the following zymography according to our test, which was similar with Ma et al. (2017). The position of the UV lamp, the camera (Sony α 6000, Sony Inc.) and the samples was fixed (Fig. S2). The fluorescent intensity of the substrate is proportional to the enzyme activity under UV light.

To quantify the zymogram images, a standard calibration that relates the activities of various enzymes to zymogram fluorescence (i.e., fluorescence of the saturated membrane) is required. The calibration was established by adding 15 μL of the MUF-the fluorescent tag substrate solution at concentrations of 0.01, 0.2, 0.5,1, 2, 4, 6, and 10 mM to the 2 × 2 cm membrane. The area of the MUF diffusion was calculated by ImageJ (National Institutes of Health). The membranes used for calibration were imaged under UV light and analyzed in the same manner as the samples (Guber et al., 2018). The processed 16-bit grayscale images were used for further analysis. We calculated the average enzyme activity on the soil profile of the membrane application area to compare the effects of the amendments on soil enzyme activity. The data are shown in Table S1.

To qualify the capacity of roots and microbes to immobilize nutrients and utilize C, the rhizosphere and the extent of bulk soil hotspots of enzyme activities were also calculated based on zymograms (Figs. S5 and S6). Bulk soil hotspots were defined as regions in the bulk soil where enzyme activities are much higher compared to the average soil conditions (i.e., very bright regions in the bulk soil of each zymogram) (Yakov and Blagodatskaya, 2015). The bulk soil hotspots extent of enzyme activities was calculated to indicate the impact of manure and biochar application on soil microbes and to compare with the rhizosphere extent of enzyme activities. Briefly, based on the actual size of the membrane (M), the size of each pixel (E) was calculated by drawing a line along one membrane side and counting the pixel number on this line (N): E = M/N. Five to six straight lines in each of the three zymogram replicates were drawn, starting from the root center or bulk soil hotspot center. Gray values from each line were extracted and the pixel numbers were recorded. Scatter-plots of distance from the root center or the bulk soil hotspot center and gray values were created. An average scatter-plot based on these 5–6 lines was then calculated. Finally, three averaged scatter-plots from three replicates of the zymogram were derived and then correlated using 4-parameter logistic regressions (Fig. S3 & S4). Gray values can be converted to enzyme activities based on the calibration line. The distance from the root/bulk soil hotspot center to the constant level of the regression curve was considered as the extent of enzyme activities.

2.4. Sample analysis

Soil water content was determined gravimetrically at 105 °C for 8 h. Soil pH was determined using a glass electrode meter (pHs −320) (ISO 10390, 2005) in a suspension of 1:5 soil/water ratio (w/v). Soil electrical conductivity (EC) was measured based on the electrode method (MEEC, 2016). The cation exchange capacity (CEC) of soil, manure and its biochar was determined by the hexamminecobalt trichloride solution-spectrophotometric method (Aran et al., 2008). The Brunauer-Emmett-Teller (BET) specific surface area was determined through nitrogen adsorption isotherm measurements (Jaroniec et al., 1998). Soil

organic carbon (SOC) was measured with a TOC analyzer coupled with SSM-5000A, and soil organic matter was calculated by multiplying SOC by a coefficient of 1.724 (CSBTS, 1988; Johnston et al., 2009). Total N (TN) was measured using the Kjeldahl method (Elsas, 1995). Total phosphorus (TP) was measured via visible light spectrophotometer (UV-6100, METASH, China) after wet digestion with ethanol and NaOH. Microbial biomass carbon (MBC) was determined using the fumigation-extraction procedure after extraction with 0.5 M K_2SO_4 (Vance et al., 1987). Total chromium and its chemical speciation were determined by flame atomic absorption spectrophotometry (Ggx-9 Haiguang Beijing) and the BCR sequential extraction procedure modified by Rauret et al. (Rauret et al., 1999; Gao et al., 2010). The concentrations of other heavy metals in digested samples were determined using ICP-MS (ELAN-6000DRC-e). Specifically, 100 mg soil samples were digested by 6 ml chloroazotic acid (mixture of HNO_3 and HCl) with a volume ratio of 3:1. Soil NO_3^--N and available P concentrations after the incubation were measured by an ultraviolet spectrophotometer (SFAC, 2016; MARAC, 2017). The main characteristics of manure and its biochar were determined accordingly. Fourier transform infrared spectrophotometry (FT-IR, IS10) was used to analyze the surface functional groups of manure and biochar before and after incubation. Briefly, after being ground and mixed thoroughly, the test powder was prepared via the KBr disk method (Shi et al., 2019). The spectra were collected in the wavenumber range from 400 cm^{-1} to 4000 cm^{-1}, with a resolution of 2 cm^{-1}. The average FT-IR spectrum was generated from 10 measurements. The FT-IR spectra were processed through baseline correction, noise reduction and normalization. Manure and biochar were picked out using a tweezer after incubation. The morphological properties (e.g., color and size) of both materials were the criteria for the separation.

2.5. Statistical analysis

Statistical analysis was performed using the SPSS 23.0 software package for Windows (SPSS Inc., Chicago, IL, USA). A one-way analysis of variance (ANOVA) and a least significant difference (LSD) multiple comparisons test ($p < 0.05$) were used to assess significant differences in soil properties, Cr chemical speciation, enzyme activity and its extent among the three treatments. Pearson correlation analysis was performed to explore the pairwise relationship between different variables (i.e., enzyme activity, heavy metals, and soil pH). The relationship between enzyme activities and the distance away from the root center or bulk soil hotspot center was correlated using a 4-parameter logistic regression. All figures were developed using Origin 9.0 (Origin Lab Inc.).

3. Results

3.1. Soil and plant characteristics

Soil samples taken from the abandoned chemical plant were highly contaminated by chromium ($Cr_{(T)}$ = 2000 ± 64 mg kg^{-1}) and the pH equaled 5.0. After incubation for 45 days, soil pH decreased for the Control, Manure and Biochar groups ($p < 0.05$, Fig. 1A). Before the shoots were cut, soil pH in the Biochar group was higher than that in the Manure group ($p < 0.05$). At day 45, soil pH in the Biochar group showed a sudden decrease and became lower compared to the pH in the Manure group. Soil pH in the Control group also experienced a strong decrease within the first 15 days and was similar to the Biochar group, but strongly decreased after shoot cutting. Rhizosphere soil pH in the Manure group was lower than bulk soil ($p < 0.05$), while the pH between the rhizosphere and bulk soil in the Control and Manure groups remained unchanged ($p > 0.05$, Fig. S5A).

Shoot biomass was higher in the Biochar group compared to the Control and Manure groups ($p < 0.05$, Fig. 1B). The maize performance index (PI) results calculated from shoot biomass showed that the Biochar group had better maize growth than the Manure group (PI_{Bio} = 2.27, PI_{Man} = 0.88). The ratio of shoot to root biomass was the highest in the Biochar group (ca. 2.32), followed by the Control (*ca.* 1.32) and Manure groups (*ca.* 0.87).

3.2. Chemical speciation of Cr

Manure and its biochar application induced significant chemical speciation dynamics of Cr (Fig. 2 and S6). Exceptions were the oxidizable and residual fractions, which were not influenced by manure and its biochar application during the whole incubation period. However, both fractions were the main speciation of Cr, which in total accounted for approximately 95% of Cr (T).

Acid soluble Cr increased over time, but the increment with time was smaller in the Manure and Biochar groups compared to the Control group (Fig. 2A). This resulted in a decline in acid soluble Cr by 10.66% and 12.38% in the Manure and Biochar groups, respectively, at day 30 compared to the Control group ($p < 0.05$). A similar decline was found at day 45 ($p < 0.05$). A negative relationship between soil pH and acid soluble Cr was also confirmed, indicating the strong impact of soil pH on the dynamics of Cr chemical speciation (Table 3). Reducible Cr increased at day 15 and then decreased again ($p < 0.05$).

At day 45, acid soluble Cr in the rhizosphere soil of the Control group was 19.25% higher compared to bulk soil (Fig. 2C). Rhizosphere soil in the Manure and Biochar groups had higher reducible Cr versus bulk soil ($p < 0.05$).

3.3. Spatio-temporal distribution of enzyme activities

By applying manure and biochar at a dose of 5 g C kg^{-1} soil, the rhizosphere extent of enzyme activities varied among the three treatments and decreased gradually from day 5 to day 30 (β-glucosidase: reduction of ca. 1.1 mm in the Control group, 0.3 mm in the Biochar group and 0.4 mm in the Manure group; phosphomonoesterase: reduction of ca. 0.4 mm in the Control group, 0.5 mm in the Biochar group and 0.2 mm in the Manure group). Negative relationships between the extent of β-glucosidase and phosphomonoesterase activities and acid soluble Cr were found ($p < 0.05$, Table 4). Manure and its biochar application reduced the rhizosphere extent compared to the Control group ($p < 0.05$; Figs. 3, 4, S7 and S8). The rhizosphere extent of β-glucosidase and phosphomonoesterase activities were the narrowest in the Manure group, followed by the Biochar and Control groups. Furthermore, the rhizosphere extent of enzyme activities were also wider than the bulk soil hotspots extent (Fig. 4). The rhizosphere extent of β-glucosidase activities ranged from 1.2 to 2.5 mm, while the range of bulk soil hotspots extent ranged from 1.0 to 1.8 mm. Phosphomonoesterase activities in the rhizosphere extended from 1.3 to 1.9 mm, but its activities in bulk soil hotspots ranged from 1.1 to 1.8 mm.

A positive relationship between average N-acetyl-glucosaminidase and β-glucosidase activities on soil profile and soil pH was found ($p < 0.05$, Table 3), while phosphomonoesterase had no significant relation with soil pH. β-glucosidase and phosphomonoesterase were both negatively correlated with acid soluble Cr ($p < 0.05$). Further, N-acetyl-glucosaminidase was positively correlated with the reducible fraction of Cr.

4. Discussion

4.1. Impact of organic amendments on soil acidification

Soil pH in the Control group strongly decreased by 0.4 units during the first 15 days of incubation and then became stable until day 30. In this process, the H^+ concentration increased by 2.5-fold, indicating that the soil became more acidic. Findings from previous studies suggested that soil acidification could result from decomposition of organic

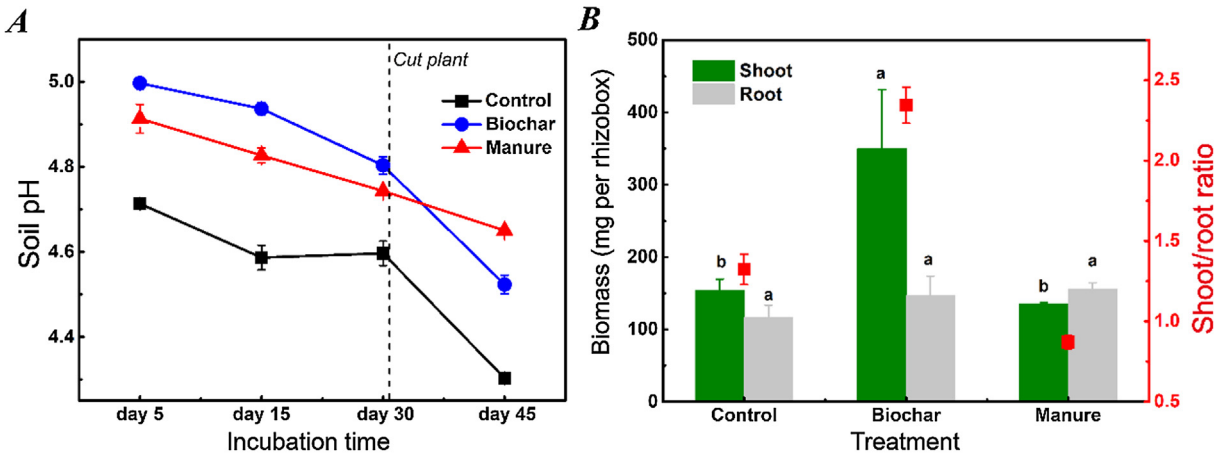

Fig. 1. A, response of soil pH to manure and its biochar application during the whole incubation period; **B**, plant biomass and shoot/root ratio. The lower-case letters represent significant differences among treatments ($p < 0.05$). Error bars represent standard error (SE). Control: a control soil without any addition. Biochar: soil homogeneously mixed with manure-derived biochar. Manure: soil homogenously mixed with cow manure.

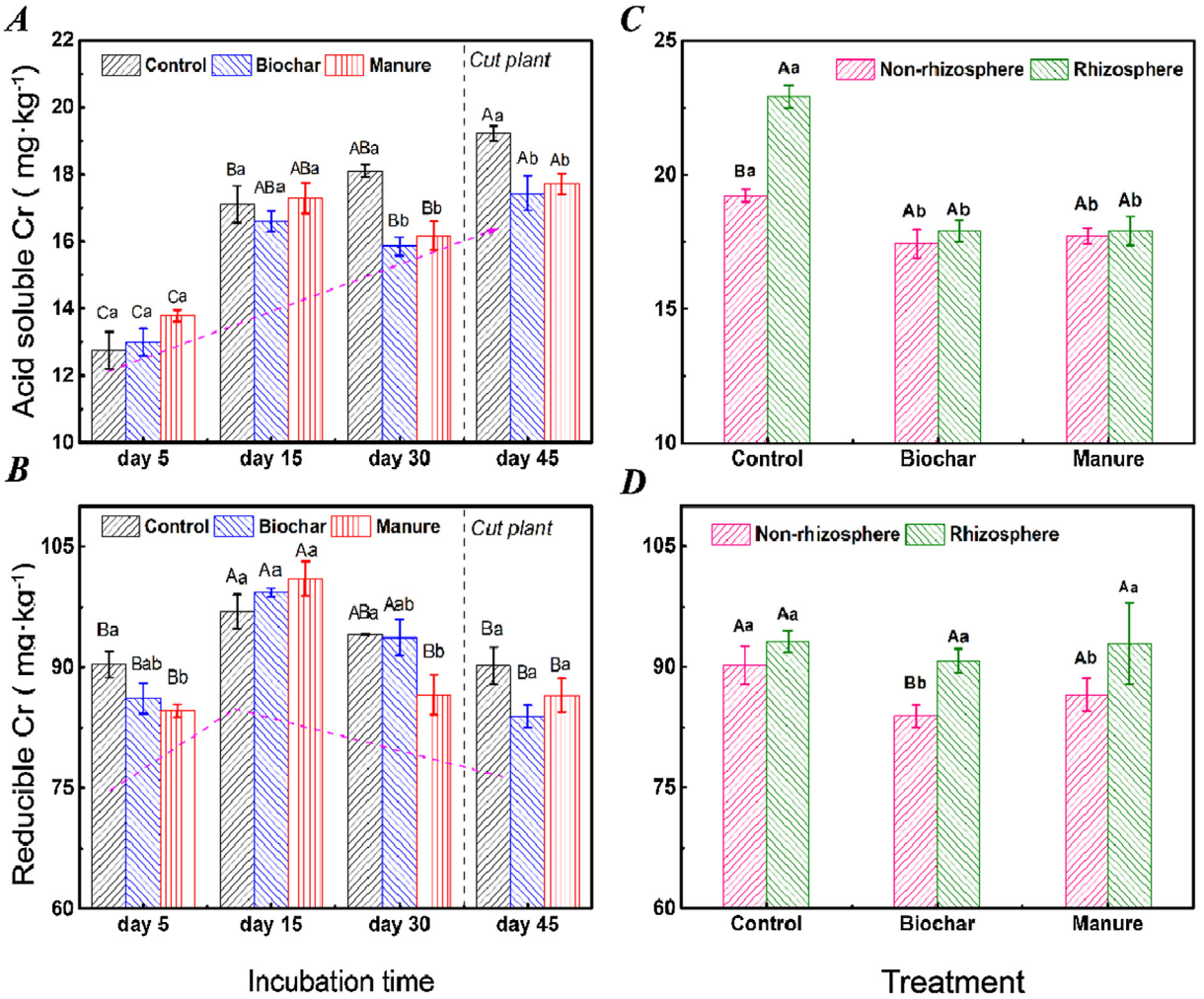

Fig. 2. A, effects of manure and its biochar application on acid soluble Cr; **B**, effects of manure and its biochar application on reducible Cr; **C**, acid soluble Cr in rhizosphere soil and non-rhizosphere soil at the end of incubation; **D**, reducible Cr in rhizosphere soil and non-rhizosphere soil at the end of incubation. Lower-case letters above the bars indicate significant differences among Control, Manure and Biochar ($p < 0.05$). Capital letters in Fig. 2C & D indicate significant differences between rhizosphere and non-rhizosphere soil ($p < 0.05$). Error bars represent standard error (± SE). Control: a control soil without any addition. Biochar: soil homogeneously mixed with manure-derived biochar. Manure: soil homogenously mixed with cow manure. Rhizosphere: rhizosphere soil. Non-rhizosphere: non-rhizosphere soil.

Table 3
Correlation coefficients between enzyme activities of soil profile and chemical speciation of Cr based on Pearson correlation.

	pH	F1	F2	F3	F4	NAG	BG	PHOS
pH	1	**−0.35***	0.24	−0.20	0.14	**0.45****	**0.38***	0.19
F1		1	0.25	**0.48****	−0.23	0.12	**−0.37***	**−0.61****
F2			1	−0.23	0.09	**0.51****	0.14	−0.13
F3				1	**−0.40****	−0.27	−0.19	−0.29
F4					1	0.29	0.18	0.32
NAG						1	0.26	0.15
BG							1	**0.64****
PHOS								1

F1–F4 represent the acid soluble, reducible, oxidizable and residue fractions of heavy metals, respectively. NAG, BG, PHOS represent the N-acetyl-glucosaminidase, β-glucosidase and phosphomonoesterase enzyme activity, respectively. Significant correlations were shown in **Bold**.
*Significant at $p < 0.05$.
**Significant at $p < 0.01$.

Table 4
Correlation coefficients between rhizosphere or bulk soil hotspot extent of enzyme activities and soil pH or acid soluble Cr based on Pearson correlation.

	NAG		BG		PHOS	
	Rhizosphere	Bulk soil	Rhizosphere	Bulk soil	Rhizosphere	Bulk soil
pH	−0.09	0.064	−0.29	−0.11	**−0.75****	0.10
F1	−0.09	−0.15	**−0.62****	**−0.60****	**−0.47***	**−0.56****

F1 represents the acid soluble Cr. NAG, BG, PHOS represent the N-acetyl-glucosaminidase, β-glucosidase and phosphomonoesterase activity, respectively. "Rhizosphere" represents the rhizosphere extent of enzyme activities; "Bulk soil" represents the bulk soil hotspots extent of enzyme activities. Significant correlations were shown in **Bold**.
*Significant at $p < 0.05$.
**Significant at $p < 0.01$.

matter, release of carbon dioxide or plant root exudation (Lu et al., 2005; Kabatapendias, 2010). Manure and its biochar application significantly increased soil pH (Fig. 1A). The liming effect of biochar generally depends on its feedstock and the pyrolysis temperature, and more generally relates to the base concentration of the ash. In this study, biochar application induced a greater pH increase compared to its feedstock before plant cutting, indicating that the liming effect of biochar was enhanced compared to its feedstock (Yuan et al., 2011). This enhancement was mainly attributed to the larger pH, ash content and BET specific surface area (Gomez-Eyles et al., 2013) in the manure-derived biochar (Table 2). A continuous reduction in soil pH was found in the three treatments after plant cutting at day 30. This could be because of the decomposition of plant root residues, which will release some organic functional groups, dissociate H^+ and accelerate soil acidification (Rukshana et al., 2009; Weil and Brady, 2016; Liu et al., 2018).

Biochar application induced lower rhizosphere soil pH in contrast to the bulk soil ($p < 0.05$, Fig. S5A). Maize performance index, as calculated in this study, was higher in the Biochar group compared to the Manure group, indicating that maize growth is improved with biochar application (Kanchikerimath and Singh, 2001). This induced greater release of root exudates in the Biochar group, which partly consist of organic acids, amino acids and fatty acids (Antoniadis et al., 2017a). The lower rhizosphere soil pH may be attributed to the residues of root exudates compared to the Manure and Control groups. Despite the non-significant difference between the pH values of rhizosphere and non-rhizosphere soil in the Manure and Control groups, a slightly decreased pH in rhizosphere soil was demonstrated (Fig. S5A). This result agrees well with a previous review study (Kuzyakov and Razavi, 2019), which stated that the gradient of soil pH between the root surface and non-rhizosphere soil decreases with decreasing soil pH. Even though the application of manure and its biochar attempted to neutralize soil acidity, the soil still remained acidic throughout the whole incubation period for the treatment duration. This will influence the bioavailability of chromium, microbial and enzyme activities, and plant growth.

4.2. Cr concentration and speciation in soil

Acid soluble Cr content was negatively correlated with soil pH ($p < 0.05$, Table. 3). Although acid soluble Cr increased with time, the application of manure and biochar slowed down the increasing rate by 47% and 55%, respectively, which supported our first hypothesis. Previous studies have indicated that soil pH played an important role in controlling the geochemical behavior of heavy metals in soil solid and liquid phases (Pietrzykowski et al., 2014). The geochemical behavior of Cr was greatly affected by soil pH and redox potential (Ashraf et al., 2017). According to the Eh-pH diagram of the chromium system ($C_{T,Cr}$ = 10E-4 mol·L^{-1}), when the soil is acidic and the redox potential is low, soil Cr mainly exists in the state of Cr(III) (Yuan et al., 2011). This was consistent with our results, showing that the oxidizable Cr was one of the main fractions in the acidified soil and was positively correlated with acid soluble Cr ($p < 0.01$). However, Cr(III) has low solubility only at pH < 5.5 (Choppala et al., 2018), indicating that Cr(III) was almost precipitated, very stable and thus less toxic in severely acidified soil.

Manure and its biochar application not only mitigated soil acidification but also altered the chemical speciation of Cr through adsorption and complexation (Agegnehu et al., 2017). Animal manure contains substantial biodegradable organic matter which has a large number of oxygen-containing functional groups (Yang et al., 2018a). These functional groups can immobilize Cr ions and change their chemical fraction (Dai et al., 2017; Zhu et al., 2017). For instance, organic amendments caused Cr detoxification by reducing Cr(VI) to Cr(III) and subsequent precipitation as chromic hydroxide (Park et al., 2011). After pyrolysis, the amount and species of oxygen-containing functional groups in biochar increased, which enhanced the capacity to adsorb and immobilize inorganic and organic pollutants from contaminated soil (Zhou et al., 2019). In this study, compared with manure, the new peaks at 795 cm^{-1} and 465 cm^{-1} appearing in biochar corresponded to C-N and Fe-O (Fig. 5A)(Yang et al., 2018b). After incubation, manure and its biochar were separated from soil and their FT-IR spectra were recorded. The new peaks at 774 cm^{-1} (Fig. 5B) were intrinsic vibrations of the Cr–O bonds, respectively (Bhaumik et al., 2011). This was indicative of the adsorption of Cr onto manure and its biochar. Furthermore, plant roots secrete organic acids during growth and degradation processes, which can also affect the chemical speciation of Cr (Hinsinger et al., 2003).

4.3. Impact of organic amendments on plant characteristics

A performance index (PI) equal to or lower than 1.0 indicates that the amendment has no impact on improving plant growth. Therefore, the dramatically increased PI induced by manure-derived biochar, instead of manure, demonstrated that biochar application prompts plant growth in Cr-contaminated soil. A control group without Cr contamination is necessary to confirm Cr toxicity on plant growth and the mitigation of biochar application for Cr toxicity, but it is not possible to find soil uncontaminated by Cr from or close to the sampling field. Nevertheless, previous studies have stated that Cr application in soil strongly depressed maize growth (e.g., decreased plant biomass, length, grain protein) (Maiti et al., 2012; Rizvi and Khan, 2018). According to FT-IR analysis results, the new peaks appearing in biochar also indicated the enhanced capacity of biochar to adsorb Cr and remediate hexavalent Cr toxicity (Fig. 5A). Some environmental factors have also been proposed to modify plant biomass allocation patterns, such as nutrient levels, warming, precipitation gradients, etc. (Sun and Wang,

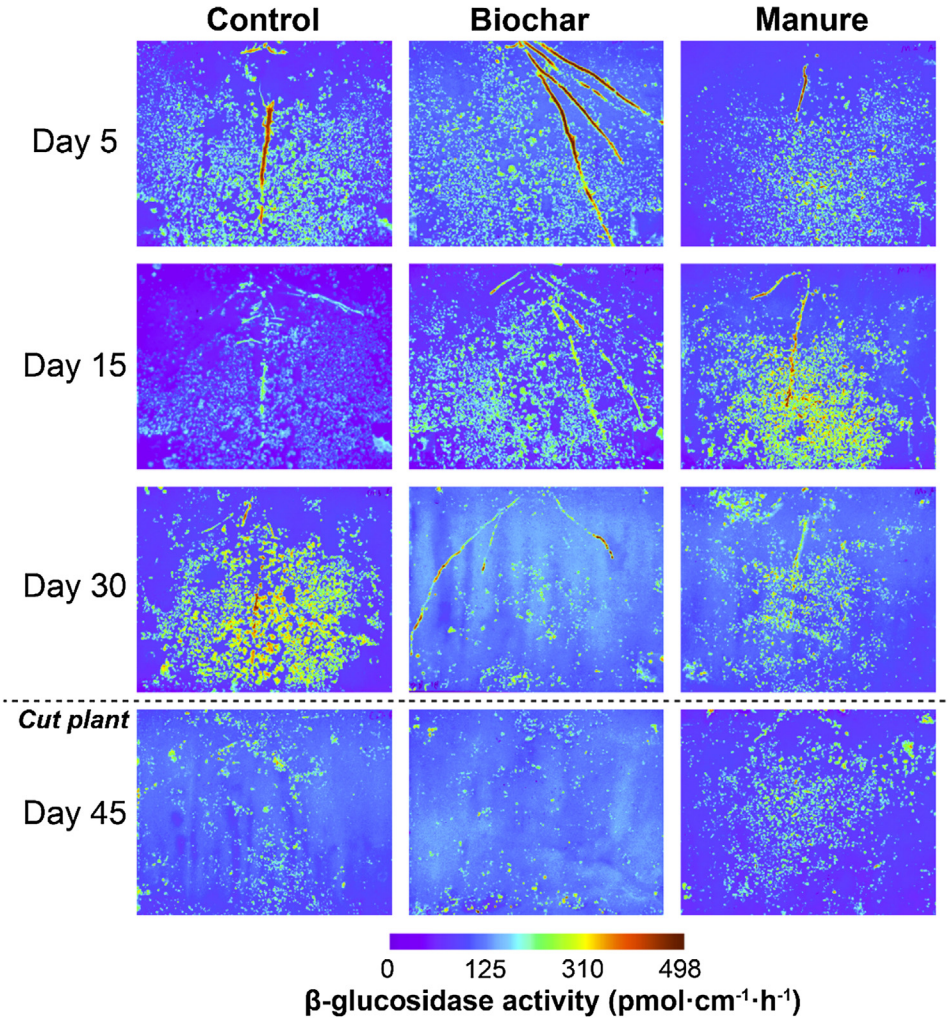

Fig. 3. Examples of zymograms for β-glucosidase activities. The actual images of soil profile at day 30 were shown in Fig. S9. Three rows represent response of activities to three treatments: 1) Control, 2) Biochar and 3) Manure. Figures from top to bottom are the measurements at days 5, 15, 30 and 45. The color bar corresponds to β-glucosidase activity (pmol·cm^{-2}h^{-1}). Control: a control soil without any addition. Biochar: soil homogeneously mixed with manure-derived biochar. Manure: soil homogenously mixed with cow manure.

2016). Manure allocated many nutrients and easily available organic matter to soil, but a strong competition for nutrients between plants and microbes may limit nutrient uptake and depress plant growth (Liu et al., 2017). The lowest shoot to root ratio (i.e., shoot/root ratio = 0.87 < 1.0) in the Manure group demonstrated that manure application caused a wasteful competition between plant and microbes (Biedrzycki et al., 2010). In contrast, biochar application induced larger average enzyme activities on soil profile than control soil, indicating that organic matter decomposition in the Biochar group was stronger than the Control group. This will result in more release of available nutrients and support plant growth (Flanagan and van Cleve, 1983; Muscolo et al., 2007). Our results also show that soil NO_3^--N, being more preferred by maize (Daryanto et al., 2019), and available P concentrations are higher in the Biochar group compared to the Control group (Table S2). With an abundant nutrient supply from soil, photosynthates will accumulate more in shoots instead of roots (Gan et al., 2001; Mašková and Herben, 2018). Our results also supported the "optimal partitioning" theory in biomass allocation of plants, i.e., that plants respond to variable environmental conditions by allocating biomass among various organs to capture nutrients and light to maximize their growth rate (McConnaughay and Coleman, 1999; Shipley and Meziane, 2002).

In contrast to the strongly increased shoot biomass, root biomass in the Biochar group had no significant difference between the Control and Manure groups. This may be attributed to a specific characteristic of Cr, i.e., that chromium retention inside the roots is a well-documented plant defense mechanism (Shahid et al., 2017). Soil pH in all treatments was less than 5, which is not favorable for maize root growth. Previous studies demonstrated that Cr application at a concentration of 50–204 mg kg^{-1} seriously depressed root growth and development, with a decrease in root biomass by 45–61% (Mallick et al., 2010; Karthik et al., 2016; Rizvi and Khan, 2019). In this study, plants showed strong withering at day 30: leaves turned yellow and roots began apoptosis, which may be exacerbated by Cr in the soil (Fig. S9).

4.4. Impact of organic amendments on enzyme activities and their extent

The rhizosphere and bulk soil hotspots extent of β-glucosidase and phosphomonoesterase showed a strong decrease with time for three treatments (Fig. 4); the rate of such a decrement is reduced in the Biochar and Manure groups. The rhizosphere and bulk soil hotspots extent of enzyme activities generally indicates the capacity of roots and microorganisms to immobilize nutrients and utilize carbon (Razavi et al., 2016). Therefore, the decreased extent demonstrated weakening root growth and microbial activities. Soil pH could be responsible for this weakening effect as our results illustrated that its extent decreased in parallel with decreasing soil pH and increasing acid soluble Cr (Fig. 1, Table 4).

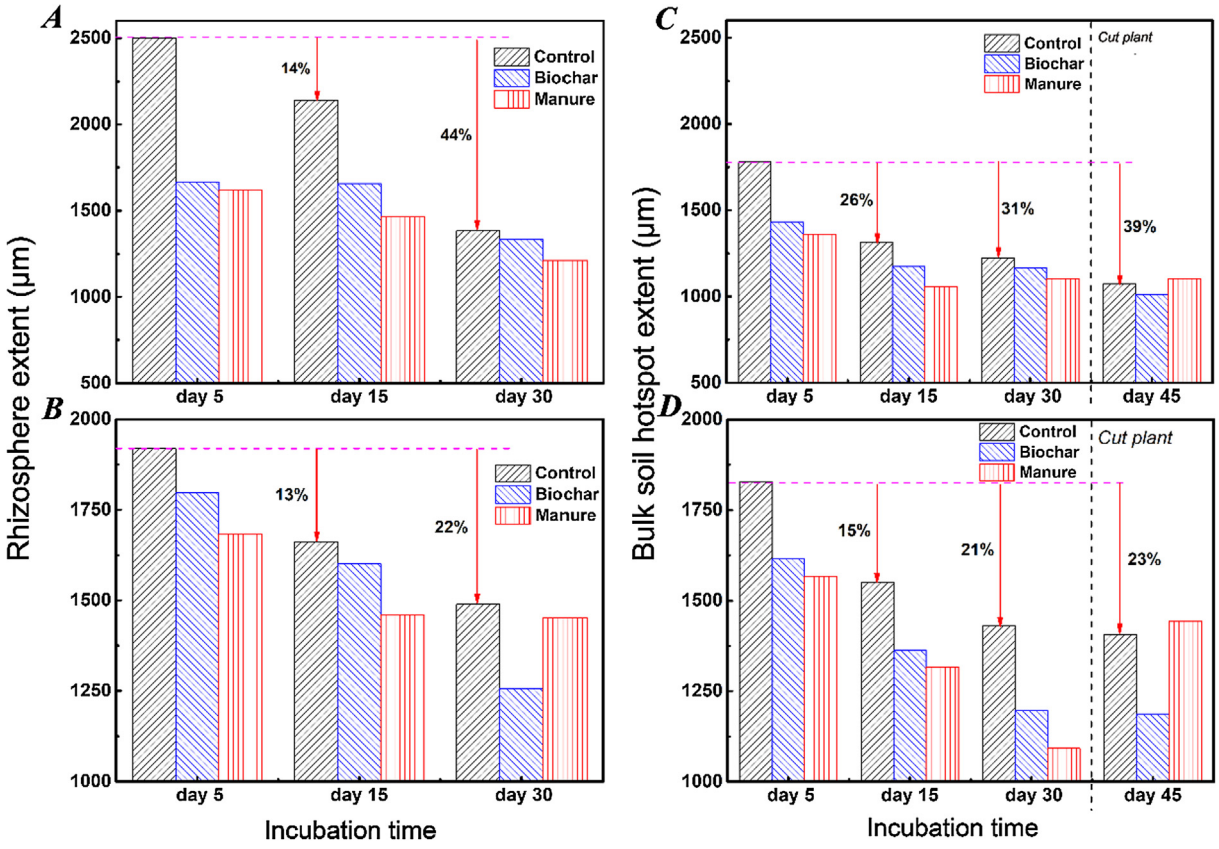

Fig. 4. A, rhizosphere extent of β-glucosidase activity; **B**, rhizosphere extent of phosphomonoesterase activity; **C**, bulk soil hotspot extent of β-glucosidase activity; **D**, bulk soil hotspots extent of phosphomonoesterase activity. All the data were derived from logistic regression curve of enzyme activity as a function of distance from root center or bulk soil hotspots. The values beside the red line show the decreasing percentage of the extent of enzyme activities with time in Control. Control: a control soil without any addition. Biochar: soil homogeneously mixed with manure-derived biochar. Manure: soil homogenously mixed with cow manure. (For interpretation of the references to color in this figure legend, the reader is referred to the web version of this article.)

Soil enzyme activities were also strongly affected by pH, which is in accordance with a previous study (Turner, 2010). Both β-glucosidase and N-acetyl-glucosaminidase activities were inhibited with decreasing soil pH (Table 3). The exceptional non-significant relationship between soil pH and phosphomonoesterase activity may be induced by the co-effect of acid phosphatase and alkaline phosphatase because both enzymes coexist in soil and have varied optimum pH activities (Acosta-Martínez et al., 2011). Further, negative relationships between enzyme activities and acidic soluble Cr also indicated that the enhanced bioavailability of Cr under acidic conditions may constrain enzyme

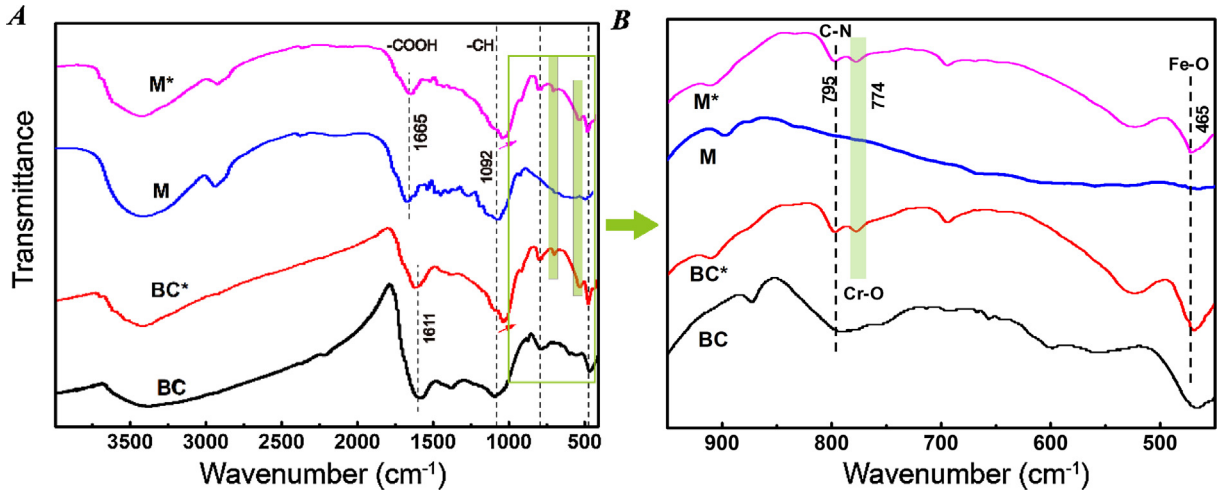

Fig. 5. A, The FTIR spectrum of manure and biochar before and after their application into Cr-contaminated soil; **B**, magnified fragments spectra in the range of 1000 – 400 cm^{-1} recorded before and after application. M: manure before the incubation. M*: manure after the incubation. BC: biochar before the incubation. BC*: biochar after the incubation. The green bars show the presence of Cr-O in manure and biochar after the incubation. The dashed vertical lines mark the positions of some functional groups such as –COOH, –CH, C–N and Fe-O. (For interpretation of the references to color in this figure legend, the reader is referred to the web version of this article.)

activities. One exception is that we found a positive relationship between N-acetyl-glucosaminidase and the reducible fraction of Cr. This Cr fraction is generally bound to Fe/Mn oxides. Fe oxides may act as an electron acceptor and enhance nitrification processes with a limited oxygen supply (Liptzin and Silver, 2009; Huang et al., 2016). This will cause decreased inorganic nitrogen (NH_4^+), which subsequently accelerates the production of N-cycling related enzymes (i.e., N-acetyl-glucosaminidase). The enhanced nitrification process could also contribute to the decreased soil pH because H^+ will be released to acidify soil (He et al., 2012).

The rhizosphere extent of β-glucosidase and phosphomonoesterase activities was wider than the bulk soil hotspots extent of both enzymes. This result supported our second hypothesis. Plants roots not only exude various organic compounds but also release enzymes to decompose organic matter within their rhizospheres. Further, microorganisms in this area also become more active due to the impact of rhizodeposits. Therefore, a wider rhizosphere extent was engendered. Among treatments, manure application resulted in the narrowest rhizosphere and bulk soil hotspots extent of β-glucosidase and phosphomonoesterase activities, followed by the Biochar and Control groups. This was in accordance with our third hypothesis. The narrowest extent of this observation can be explained by the addition of labile organic compounds and nutrients following the manure application (Kuzyakov and Razavi, 2019). With abundant resources for growth and maintenance, microbes and plant roots do not necessarily extend enzymes very far.

5. Conclusions

For the first time, we identified and compared the impact of manure and its biochar application on the spatiotemporal distribution of soil enzyme activities under the stress of Cr contamination. Soil pH dramatically decreased during 45 days of incubation, which strongly increased the acid soluble fraction of Cr, decreased the activities of β-glucosidase and N-acetyl-glucosaminidase ($p < 0.05$), and narrowed the rhizosphere extent of enzyme activities by 13–44% compared to day 5. This indicated that the increased Cr bioavailability decreased soil microbial activities. Biochar application caused a larger liming impact compared to manure application because of the larger initial pH, ash content and BET specific surface area in manure-derived biochar. Biochar group also had the highest soil NO_3^--N and available P concentration. In addition, the greatest shoot/root ratio was also found when biochar was applied, which reduced the wasteful competition between plants and microbes in Cr-contaminated soil. The rhizosphere extent of enzyme activities (ca. 1.2–2.5 mm) was wider in comparison with the bulk soil hotspots extent (ca. 1.0–1.8 mm), indicating higher demand for low-molecular-weight compounds and nutrients in the rhizosphere by roots and microbes. Further, manure application resulted in the narrowest extent of β-glucosidase and phosphomonoesterase activities compared to the Biochar and Control groups. This could be due to the addition of labile organic compounds and nutrients following manure application. Our study emphasizes the important role of pH on Cr bioavailability and enzyme activities and demonstrates that biochar application is more suited for remediating Cr-contaminated soil.

Declaration of Competing Interest

The authors declare that there is no conflict of interests regarding the publication of this paper.

Acknowledgement

This study was supported by the National Science Foundation of China (Nos: 41807091, 41772264), the Research Fund of State Key Laboratory of Geohazard Prevention and Geoenvironment Protection (No: SKLGP2018Z001) and the Applied Basic Research Programs of Science and Technology Department of Sichuan Province (Nos: 2019YJ0507; 18YYJC1745). We acknowledge the assistance from Ying Zhang and Lingling He during the sample sampling and analysis.

Appendix A. Supplementary data

Supplementary data to this article can be found online at https://doi.org/10.1016/j.envint.2019.105277.

References

Abbas, A., Azeem, M., Naveed, M., Latif, A., Bashir, S., Ali, A., Bilal, M., Ali, L., 2019. Synergistic use of biochar and acidified manure for improving growth of maize in chromium contaminated soil. Int. J. Phytorem. 1–10. https://doi.org/10.1080/15226514.2019.1644286.

Abdu, N., Abdullahi, A.A., Abdulkadir, A., 2016. Heavy metals and soil microbes. Environ. Chem. Lett. 15, 65–84. https://doi.org/10.1007/s10311-016-0587-x.

Acostamartínez, V., Tabatabai, M.A., 2011. Phosphorus cycle enzymes. Meth. Soil Enzymol. 79415, 161–183. https://doi.org/10.2136/sssabookser9.c8.

Agegnehu, G., Srivastava, A.K., Bird, M.I., 2017. The role of biochar and biochar-compost in improving soil quality and crop performance: a review. Appl. Soil Ecol. 119, 156–170. https://doi.org/10.1016/j.apsoil.2017.06.008.

Antoniadis, V., Levizou, E., Shaheen, S.M., Ok, Y.S., Sebastian, A., Baum, C., Prasad, M.N.V., Wenzel, W.W., Rinklebe, J., 2017a. Trace elements in the soil-plant interface: phytoavailability, translocation, and phytoremediation-a review. Earth Sci. Rev. 171, 621–645. https://doi.org/10.1016/j.earscirev.2017.06.005.

Antoniadis, V., Polyzois, T., Golia, E.E., Petropoulos, S.A., 2017b. Hexavalent chromium availability and phytoremediation potential of Cichorium spinosum as affect by manure, zeolite and soil ageing. Chemosphere 171, 729–734. https://doi.org/10.1016/j.chemosphere.2016.11.146.

Antoniadis, V., Zanni, A.A., Levizou, E., Shaheen, S.M., Dimirkou, A., Bolan, N., Rinklebe, J., 2018. Modulation of hexavalent chromium toxicity on Omicronriganum vulgare in an acidic soil amended with peat, lime, and zeolite. Chemosphere 195, 291–300. https://doi.org/10.1016/j.chemosphere.2017.12.069.

Aran, D., Maul, A., Masfaraud, J.-F., 2008. A spectrophotometric measurement of soil cation exchange capacity based on cobaltihexamine chloride absorbance. C.R. Geosci. 340, 865–871. https://doi.org/10.1016/j.crte.2008.07.015.

Ashraf, A., Bibi, I., Niazi, N.K., Ok, Y.S., Murtaza, G., Shahid, M., Kunhikrishnan, A., Li, D., Mahmood, T., 2017. Chromium(VI) sorption efficiency of acid-activated banana peel over organo-montmorillonite in aqueous solutions. Int. J. Phytoremediation 19, 605–613. https://doi.org/10.1080/15226514.2016.1256372.

Bais, H.P., Weir, T.L., Gilroy, L.G., Vivanco, S.J.M., 2006. The role of root exudates in rhizosphere interactions with plants and other organisms. Annu. Rev. Plant Biol. 57, 233–266. https://doi.org/10.1146/annurev.arplant.57.032905.105159.

Bhaumik, M., Maity, A., Srinivasu, V.V., Onyango, M.S., 2011. Enhanced removal of Cr (VI) from aqueous solution using polypyrrole/Fe_3O_4 magnetic nanocomposite. J. Hazard. Mater. 190, 381–390. https://doi.org/10.1016/j.jhazmat.2011.03.062.

Biedrzycki, M.L., Jilany, T.A., Dudley, S.A., Bais, H.P., 2010. Root exudates mediate kin recognition in plants. Commun. Integrative Biol. 3, 28–35. https://doi.org/10.4161/cib.3.1.10118.

Carpio, M.I.E., Ansari, A., Rodrigues, D.F., 2018. Relationship of biodiversity with heavy metal tolerance and sorption capacity: a meta-analysis approach. Environ. Sci. Technol. 52, 184–194. https://doi.org/10.1021/acs.est.7b04131.

Choppala, G., Kunhikrishnan, A., Seshadri, B., Park, J.H., Bush, R., Bolan, N., 2018. Comparative sorption of chromium species as influenced by pH, surface charge and organic matter content in contaminated soils. J. Geochem. Explor. 184, 255–260. https://doi.org/10.1016/j.gexplo.2016.07.012.

Criquet, S., Braud, A., Neble, S., 2007. Short-term effects of sewage sludge application on phosphatase activities and available P fractions in Mediterranean soils. Soil Biol. Biochem. 39, 921–929. https://doi.org/10.1016/j.soilbio.2006.11.002.

CSBTS (State Bureau of Technical Supervision), 1988. Method for determination of soil organic matter: NY/T pp. 85–88.

Dai, Z., Zhang, X., Tang, C., Muhammad, N., Wu, J., Brookes, P.C., Xu, J., 2017. Potential role of biochars in decreasing soil acidification – a critical review. Sci. Total Environ. 581–582, 601–611. https://doi.org/10.1016/j.scitotenv.2016.12.169.

Daryanto, S., Wang, L.X., Gilhooly, W.P., Jacinthe, P.A., 2019. Nitrogen preference across generations under changing ammonium nitrate ratios. J. Plant Ecol. 12, 235–244. https://doi.org/10.1093/jpe/rty014.

Dinesh, R., Dubey, R.P., Prasad, G.S., 1998. Soil microbial biomass and enzyme activities as influenced by organic manure incorporation into soils of a rice-rice system. J. Agron. Crop Sci.-Zeitschrift Fur Acker Und Pflanzenbau 181, 173–178. https://doi.org/10.1111/j.1439-037X.1998.tb00414.x.

Duan, C., Fang, L., Yang, C., Chen, W., Cui, Y., Li, S., 2018. Reveal the response of enzyme activities to heavy metals through in situ zymography. Ecotoxicol. Environ. Saf. 156, 106–115. https://doi.org/10.1016/j.ecoenv.2018.03.015.

Eivazi, F., Tabatabai, M.A., 1977. Phosphatases in soils. Soil Biol. Biochem. 9, 167–172. https://doi.org/10.1016/0038-0717(77)90070-0.

Ekschmitt, K., Liu, M.Q., Vetter, S., Fox, O., Wolters, V., 2005. Strategies used by soil biota to overcome soil organic matter stability – why is dead organic matter left over in the soil? Geoderma 128, 167–176. https://doi.org/10.1016/j.geoderma.2004.12.024.

Elsas, J.D.V., 1995. Methods of soil analysis. Part 2 — microbiological and biochemical

properties. Sci. Hortic. 63, 131–133. https://doi.org/10.1016/0304-4238(95)90023-3.
Ertani, A., Mietto, A., Borin, M., Nardi, S., 2017. Chromium in agricultural soils and crops: a review. Water Air Soil Pollut. 228. https://doi.org/10.1007/s11270-017-3356-y.
Flanagan, P.W., Van Cleve, K., 1983. Nutrient cycling in relation to decomposition and organic-matter quality in taiga ecosystems. Can. J. For. Res. 13, 795–817. https://doi.org/10.1139/x83-110.
Gan, Y., Stulen, I., Posthumus, F., Keulen, H. Van, Pieter, J.C., 2002. Effects of N management on growth, N_2 fixation and yield of soybean. Nutr. Cycl. Agroecosyst. 62, 163–174. https://doi.org/10.1023/A:1015528132642.
Gao, X., Chen, C.-T.A., Wang, G., Xue, Q., Tang, C., Chen, S., 2010. Environmental status of Daya Bay surface sediments inferred from a sequential extraction technique. Estuarine Coastal and Shelf. Science 86, 369–378. https://doi.org/10.1016/j.ecss.2009.10.012.
German, D.P., Weintraub, M.N., Grandy, A.S., Lauber, C.L., Rinkes, Z.L., Allison, S.D., 2012. Optimization of hydrolytic and oxidative enzyme methods for ecosystem studies (vol 43, pg 1387, 2011). Soil Biol. Biochem. 44, 151. https://doi.org/10.1016/j.soilbio.2011.11.002.
Ghosh, U., Luthy, R.G., Cornelissen, G., Werner, D., Menzie, C.A., 2011. In-situ sorbent amendments: a new direction in contaminated sediment management. Environ. Sci. Technol. 45, 1163. https://doi.org/10.1021/es102694h.
Gomez-Eyles, J.L., Beesley, L., Moreno-Jimenez, E., Ghosh, U., Sizmur, T., 2013. The potential of biochar amendments to remediate contaminated soils. Biochar. Soil Biota 100–133. https://doi.org/10.1201/b14585.
Guber, A., Kravchenko, A., Razavi, B.S., Uteau, D., Peth, S., Blagodatskaya, E., Kuzyakov, Y., 2018. Quantitative soil zymography: mechanisms, processes of substrate and enzyme diffusion in porous media. Soil Biol. Biochem. 127, 156–167. https://doi.org/10.1016/j.soilbio.2018.09.030.
He, J.Z., Hu, H.W., Zhang, L.M., 2012. Current insights into the autotrophic thaumarchaeal ammonia oxidation in acidic soils. Soil Biol. Biochem. 55, 146–154. https://doi.org/10.1016/j.soilbio.2012.06.006.
Hinsinger, P., Bengough, A.G., Vetterlein, D., Young, I.M., 2009. Rhizosphere: biophysics, biogeochemistry and ecological relevance. Plant Soil 321, 117–152. https://doi.org/10.1007/s11104-008-9885-9.
Hinsinger, P., Plassard, C., Tang, C.X., Jaillard, B., 2003. Origins of root-mediated pH changes in the rhizosphere and their responses to environmental constraints: a review. Plant Soil 248, 43–59. https://doi.org/10.1023/a:1022371130939.
Hoang, D.T.T., Razavi, B.S., Kuzyakov, Y., Blagodatskaya, E., 2016. Earthworm burrows: kinetics and spatial distribution of enzymes of C-, N- and P- cycles. Soil Biol. Biochem. 99, 94–103. https://doi.org/10.1016/j.soilbio.2016.04.021.
Huang, G., 2012. Chitinase inhibitor allosamidin and its analogues: an update. Curr. Org. Chem. 16, 115–120. https://doi.org/10.2174/138527212798993121.
Huang, X., Zhu-Barker, X., Horwath, W.R., Faeflen, S.J., Luo, H., Xin, X., Jiang, X., 2016. Effect of iron oxide on nitrification in two agricultural soils with different pH. Biogeosciences 13, 5609–5617. https://doi.org/10.5194/bg-13-5609-2016.
ISO 10390, 2005. Soil quality—determination of pH (ISO 10390: 2005). Available at: https://www.iso.org/standard/40879.html.
Jaroniec, M., Kruk, M., Sayari, A., 1998. Adsorption methods for characterization of surface and structural properties of mesoporous molecular sieves. Studies Surf. Sci. Catal. Elsevier Masson SAS. https://doi.org/10.1016/S0167-2991(98)81008-2.
Johnston, A.E., Poulton, P.R., Coleman, K., 2009. Chapter 1 Soil Organic Matter. Its Importance in Sustainable Agriculture and Carbon Dioxide Fluxes, 1st ed, Advances in Agronomy. Elsevier Inc. https://doi.org/10.1016/S0065-2113(08)00801-8.
Kabatapendias, A., 2010. Trace Elements in Soils and Plants. Crc Press/Taylor & Francis Group:, Boca Raton, FL, USA, pp. 548.
Kanchikerimath, M., Singh, D., 2001. Soil organic matter and biological properties after 26 years of maize-wheat-cowpea cropping as affected by manure and fertilization in a Cambisol in semiarid region of India. Agric. Ecosyst. Environ. 86, 155–162. https://doi.org/10.1016/S0167-8809(00)00280-2.
Karthik, C., Oves, M., Thangabalu, R., Sharma, R., Santhosh, S.B., Arulselvi, P.I., 2016. Cellulosimicrobium funkei-like enhances the growth of Phaseolus vulgaris by modulating oxidative damage under Chromium(VI) toxicity. J. Adv. Res. 7, 839–850. https://doi.org/10.1016/j.jare.2016.08.007.
Kuzyakov, Y., Razavi, B.S., 2019. Rhizosphere size and shape: temporal dynamics and spatial stationarity. Soil Biol. Biochem. 135, 343–360. https://doi.org/10.1016/j.soilbio.2019.05.011.
Li, H., Dong, X., da Silva, E.B., de Oliveira, L.M., Chen, Y., Ma, L.Q., 2017. Mechanisms of metal sorption by biochars: biochar characteristics and modifications. Chemosphere 178, 466–478. https://doi.org/10.1016/j.chemosphere.2017.03.072.
Liptzin, D., Silver, W.L., 2009. Effects of carbon additions on iron reduction and phosphorus availability in a humid tropical forest soil. Soil Biol. Biochem. 41, 1696–1702. https://doi.org/10.1016/j.soilbio.2009.05.013.
Liu, S., Razavi, B.S., Su, X., Maharjan, M., Zarebanadkouki, M., Blagodatskaya, E., Kuzyakov, Y., 2017. Spatio-temporal patterns of enzyme activities after manure application reflect mechanisms of niche differentiation between plants and microorganisms. Soil Biol. Biochem. 112, 100–109. https://doi.org/10.1016/j.soilbio.2017.05.006.
Liu, S., Schleuss, P.M., Kuzyakov, Y., 2018. Responses of degraded Tibetan *Kobresia* pastures to N addition. Land Degrad. Dev. 29, 303–314. https://doi.org/10.1002/ldr.2720.
Lu, A., Zhang, S., Shan, X.Q., 2005. Time effect on the fractionation of heavy metals in soils. Geoderma 125, 225–234. https://doi.org/10.1016/j.geoderma.2004.08.002.
Ma, X., Razavi, B.S., Holz, M., Blagodatskaya, E., Kuzyakov, Y., 2017. Warming increases hotspot areas of enzyme activity and shortens the duration of hot moments in the root-detritusphere. Soil Biol. Biochem. 107, 226–233. https://doi.org/10.1016/j.soilbio.2017.01.009.
Ma, X., Zarebanadkouki, M., Kuzyakov, Y., Blagodatskaya, E., Pausch, J., Razavi, B.S., 2018. Spatial patterns of enzyme activities in the rhizosphere: effects of root hairs and root radius. Soil Biol. Biochem. 118, 69–78. https://doi.org/10.1016/j.soilbio.2017.12.009.
Maiti, S., Ghosh, N., Mandal, C., Das, K., Dey, N., Adak, M.K., 2012. Responses of the maize plant to chromium stress with reference to antioxidation activity. Brazilian Soc. Plant Physiol. 24, 203–212. https://doi.org/10.1590/S1677-04202012000300007.
Malcolm, R.E., 1983. Assessment of phosphatase activity in soils. Soil Biol. Biochem. 15, 403–408. https://doi.org/10.1016/0038-0717(83)90003-2.
Mallick, S., Sinam, G., Mishra, R.K., Sinha, S., 2010. Interactive effects of Cr and Fe treatments on plants growth, nutrition and oxidative status in Zea mays L. Ecotoxicol. Environ. Saf. 73, 987–995. https://doi.org/10.1016/j.ecoenv.2010.03.004.
MARAC (Ministry of Agriculture and Rural Affairs of China), 2017. Determination of nitrate nitrogen in soil – Ultraviolet spectrophotometry method. GB/T 32737-2016.
Mašková, T., Herben, T., 2018. Root:shoot ratio in developing seedlings: how seedlings change their allocation in response to seed mass and ambient nutrient supply. Ecol. Evol. 8, 7143–7150. https://doi.org/10.1002/ece3.4238.
McConnaughay, K.D.M., Coleman, J.S., 1999. Biomass allocation in plants: ontogeny or optimality? A test along three resource gradients. Ecology 80, 2581–2593. https://doi.org/10.2307/177242.
MEEC (Ministry of Ecology and Environment of China), 2016. Soil quality -determination of conductivity - electrode method: HJ 802-2016. Available at: http://kjs.mee.gov.cn/hjbhbz/bzwb/jcffbz/201606/t20160630_356524.shtml 2016.
Muscolo, A., Sidari, M., Mercurio, R., 2007. Influence of gap size on organic matter decomposition, microbial biomass and nutrient cycle in Calabrian pine (Pinus laricio, Poiret) stands. For. Ecol. Manage. 242, 412–418. https://doi.org/10.1016/j.foreco.2007.01.058.
Oburger, E., Gruber, B., Schindlegger, Y., Schenkeveld, W.D.C., Hann, S., Kraemer, S.M., Wenzel, W.W., Puschenreiter, M., 2014. Root exudation of phytosiderophores from soil-grown wheat. New Phytol. 203, 1161–1174. https://doi.org/10.1111/nph.12868.
Park, J.H., Lamb, D., Paneerselvam, P., Choppala, G., Bolan, N., Chung, J.W., 2011. Role of organic amendments on enhanced bioremediation of heavy metal(loid) contaminated soils. J. Hazard. Mater. 185, 549–574. https://doi.org/10.1016/j.jhazmat.2010.09.082.
Pietrzykowski, M., Socha, J., van Doorn, N.S., 2014. Linking heavy metal bioavailability (Cd, Cu, Zn and Pb) in Scots pine needles to soil properties in reclaimed mine areas. Sci. Total Environ. 470–471, 501–510. https://doi.org/10.1016/j.scitotenv.2013.10.008.
Pu, S.Y., Yan, C., Huang, H.Y., Liu, S.B., Deng, D.L., 2019. Toxicity of nano-CuO particles to maize and microbial community largely depends on its bioavailable fractions. Environ. Pollut. 255, 113245. https://doi.org/10.1016/j.envpol.2019.113248.
Rauret, G., Lopez-Sanchez, J.F., Sahuquillo, A., Rubio, R., Davidson, C., Ure, A., Quevauviller, P., 1999. Improvement of the BCR three step sequential extraction procedure prior to the certification of new sediment and soil reference materials. J. Environ. Monit. 1, 57–61. https://doi.org/10.1039/a807854h.
Razavi, B.S., Zarebanadkouki, M., Blagodatskaya, E., Kuzyakov, Y., 2016. Rhizosphere shape of lentil and maize: spatial distribution of enzyme activities. Soil Biol. Biochem. 96, 229–237. https://doi.org/10.1016/j.soilbio.2016.02.020.
Rinklebe, J., Shaheen, S.M., 2017. Geochemical distribution of Co, Cu, Ni, and Zn in soil profiles of Fluvisols, Luvisols, Gleysols, and Calcisols originating from Germany and Egypt. Geoderma 307, 122–138. https://doi.org/10.1016/j.geoderma.2017.08.005.
Rizvi, A., Khan, M.S., 2018. Heavy metal-mediated toxicity to maize: oxidative damage, antioxidant defence response and metal distribution in plant organs. Int. J. Environ. Sci. Technol. 16, 4873–4886. https://doi.org/10.1007/s13762-018-1916-3.
Rukshana, F., Butterly, C.B., Xu, J.M., Baldock, J.A., Tang, C.X., 2009. In: Molecular Environmental Soil Science at the Interfaces in the Earth's Critical Zone. Springer-Verlag, Berlin, pp. 331–333.
SFAC (State Forestry Administration of China), 2016. Phosphorus determination methods of forest soils. LY/T pp. 1232–2015.
Shahid, M., Shamshad, S., Rafiq, M., Khalid, S., Bibi, I., Niazi, N.K., Dumat, C., Rashid, M.I., 2017. Chromium speciation, bioavailability, uptake, toxicity and detoxification in soil-plant system: a review. Chemosphere 178, 513–533. https://doi.org/10.1016/j.chemosphere.2017.03.074.
Shi, M., Ying, D.-Y., Hlaing, M.M., Ye, J.-H., Sanguansri, L., Augustin, M.A., 2019. Development of broccoli by-products as carriers for delivering EGCG. Food Chem. 301, 125301. https://doi.org/10.1016/j.foodchem.2019.125301.
Shipley, B., Meziane, D., 2002. The balanced-growth hypothesis and the allometry of leaf and root biomass allocation. Funct. Ecol. 16, 326–331. https://doi.org/10.1046/j.1365-2435.2002.00626.x.
Sinsabaugh, R.L., Lauber, C.L., Weintraub, M.N., Ahmed, B., Allison, S.D., Crenshaw, C., Contosta, A.R., Cusack, D., Frey, S., Gallo, M.E., Gartner, T.B., Hobbie, S.E., Holland, K., Keeler, B.L., Powers, J.S., Stursova, M., Takacs-Vesbach, C., Waldrop, M.P., Wallenstein, M.D., Zak, D.R., Zeglin, L.H., 2008. Stoichiometry of soil enzyme activity at global scale. Ecol. Lett. 11, 1252–1264. https://doi.org/10.1111/j.1461-0248.2008.01245.x.
Spohn, M., Kuzyakov, Y., 2013. Distribution of microbial- and root-derived phosphatase activities in the rhizosphere depending on P availability and C allocation – coupling soil zymography with 14C imaging. Soil Biol. Biochem. 67, 106–113. https://doi.org/10.1016/j.soilbio.2013.08.015.
Sun, J., Wang, H., 2016. Soil nitrogen and carbon determine the trade-off of the above- and below-ground biomass across alpine grasslands, Tibetan Plateau. Ecol. Ind. 60, 1070–1076. https://doi.org/10.1016/j.ecolind.2015.08.038.
Sun, L., Qiu, F., Zhang, X., Dai, X., Dong, X., Song, W., 2008. Endophytic bacterial diversity in rice (Oryza sativa L.) roots estimated by 16S rDNA sequence analysis.

Microbial Ecol. 55, 415–424. https://doi.org/10.1007/s00248-007-9287-1.
Turner, B.L., 2010. Variation in pH optima of hydrolytic enzyme activities in tropical rain forest soils. Appl. Environ. Microbiol. 76, 6485–6493. https://doi.org/10.1128/aem.00560-10.
Vance, E.D., Brookes, P.C., Jenkinson, D.S., 1987. An extraction method for measuring soil microbial biomass C. Soil Biol. Biochem. 19, 703–707. https://doi.org/10.1016/0038-0717(87)90052-6.
Weil, R.R., Brady, N.C., 2016. Soil acidity. In: Brady, N.C., Weil, R.R. (Eds.), The Nature and Properties of Soils. Pearson Education Inc., USA, pp. 374–417.
Wei, X., Ge, T., Zhu, Z., Hu, Y., Liu, S., Li, Y., Wu, J., Razavi, B.S., 2018. Expansion of rice enzymatic rhizosphere: temporal dynamics in response to phosphorus and cellulose application. Plant Soil 1–13. https://doi.org/10.1007/s11104-018-03902-0.
Yakov, K., Blagodatskaya, E., 2015. Microbial hotspots and hot moments in soil_ concept & review. Soil Biol. Biochem. 83, 184–199. https://doi.org/10.1016/j.soilbio.2015.01.025.
Yanardağ, I.H., Zornoza, R., Bastida, F., Büyükkiliç-Yanardağ, A., García, C., Faz, A., Mermut, A.R., 2017. Native soil organic matter conditions the response of microbial communities to organic inputs with different stability. Geoderma 295, 1–9. https://doi.org/10.1016/j.geoderma.2017.02.008.
Yang, L., Bian, X., Yang, R., Zhou, C., Tang, B., 2018a. Assessment of organic amendments for improving coastal saline soil. Land Degrad. Dev. 29, 3204–3211. https://doi.org/10.1002/ldr.3027.
Yang, Y., Chen, N., Feng, C., Li, M., Gao, Y., 2018b. Chromium removal using a magnetic corncob biochar/polypyrrole composite by adsorption combined with reduction: Reaction pathway and contribution degree. Colloids Surfaces Physicochem. Eng. Asp. 556, 201–209. https://doi.org/10.1016/j.colsurfa.2018.08.035.
Yuan, J.-H., Xu, R.-K., Qian, W., Wang, R.-H., 2011. Comparison of the ameliorating effects on an acidic ultisol between four crop straws and their biochars. J. Soils Sediments 11, 741–750. https://doi.org/10.1007/s11368-011-0365-0.
Zhou, X., Qiao, M., Su, J.-Q., Wang, Y., Cao, Z.-H., Cheng, W.-D., Zhu, Y.-G., 2019. Turning pig manure into biochar can effectively mitigate antibiotic resistance genes as organic fertilizer. Sci. Total Environ. 649, 902–908. https://doi.org/10.1016/j.scitotenv.2018.08.368.
Zhu, X., Chen, B., Zhu, L., Xing, B., 2017. Effects and mechanisms of biochar-microbe interactions in soil improvement and pollution remediation: a review. Environ. Pollut. 227, 98–115. https://doi.org/10.1016/j.envpol.2017.04.032.
Zornoza, R., Moreno-Barriga, E., Acosta, J.A., Munoz, M.A., Faz, A., 2016. Stability, nutrient availability and hydrophobicity of biochars derived from manure, crop residues, and municipal solid waste for their use as soil amendments. Chemosphere 144, 122–130. https://doi.org/10.1016/j.chemosphere.2015.08.046.